ELSEVIER

PII: S0032-3861(97)00023-2

Polymer Vol. 38 No. 20, pp. 5233–5241, 1997
© 1997 Elsevier Science Ltd
Printed in Great Britain. All rights reserved
0032-3861/97/$17.00 + 0.00

On volume-recovery theory: 2. Test on Kovacs's original δ vs t data

L. C. E. Struik
DSM Research, PO Box 18, 6160 MD, Geleen, The Netherlands
(Received 1 July 1996; revised 17 October 1996)

Kovacs's volume-recovery data (PVAc; 40°C) can be described by the phenomenological volume-recovery theory within experimental error ($\pm 2 \times 10^{-5}$). The non-ideal character of the actual temperature jumps has a considerable effect on volume recovery, even in heating tests. Bounds and corrections for these non-idealities are given. © 1997 Elsevier Science Ltd.

(Keywords: volume recovery; volume relaxation; reduced time)

1. INTRODUCTION

In ref. 1 Kovacs's well known PVAc data[2,3] was discussed and it was shown that the τ_{eff} paradox does not exist and that τ_{eff} vs δ can be described by the phenomenological volume-recovery theory[4–7] within experimental error. The present paper shows that the theory equally well describes the original δ vs t curves, from which Kovacs calculated τ_{eff}.

A serious difficulty is that the experimental data were obtained with non-ideal dilatometer experiments, i.e. the temperature did not jump instantaneously from initial value T_0 to final value T but followed some transient. To make a proper comparison between theory and experiment, the deviations induced by these transients should be known. However, the transients depend on the shape and size of the dilatometer, the type of chilling liquid (water or oil), the polymer filling fraction of the dilatometer (determines thermal diffusivity) and the location within the dilatometer (outer parts respond quicker than the core). So, the transients are never known exactly; the only thing known is that the transients are finished within some time t_d of the order of minutes. So, the best we can achieve is an upper bound for the deviations; such bounds are derived in Section 2 and it is shown (Section 3) that the deviations between theory and experiment remain within these bounds.

2. THEORY

Theories for volume-recovery* have been proposed by different authors[4–7]. These theories are essentially equivalent, only the formalism varies from author to author. In this paper, we prefer to use the formalism of ref. 7 because:

- it is identical to that of the theory of linear viscoelasticity (response function formalism); so, the many results of this theory can be used directly. In this respect, the formalism has an advantage over that of the multi-parameter formalism used by Kovacs *et al.*[3,4].
- it is the most general and flexible version because no assumptions are made about the acceleration (shift) function and the volume response function (except, of course, for trivialities). Both functions can be determined freely from experiment. For example, in Section 3.2, we will arrive at shift functions which completely deviate from those predicted by the free-volume model. Furthermore, no specification whatsoever is required about the volume response function; this function simply follows from the data.

In Sections 2.2, 3.3 and 3.4 the theory will be applied to derive the upper bounds and corrections for the effect of non-ideal heating. Of course, such bounds can also be obtained from the other versions of the theory[4–6] and, actually, Kovacs considered the effect of non-ideal cooling/heating many years ago[4]. However, he considered cooling or heating at a constant *specified rate*; a bounding of the effects of an *unknown transient* of maximum duration t_d has, to the author's knowledge, never been worked out in the literature.

2.1. Basic equations

To derive the bounds for the effect of the transients (Sections 2.2, 3.3 and 3.4), we require the theory of ref. 7 in some detail. The formalism is as follows:

(a) At small deviations from equilibrium, all relaxation processes, including volume relaxation *must* become linear in the sense of Boltzmann's superposition principle[8]; for experimental evidence about linear volume-relaxation, see ref. 9. The linear response can be characterized by the unit step response $\psi(t)$, defined for an infinitesimal *ideal* temperature jump from initial temperature T_1 to final temperature T_2 (see *Figure 1*; ideal means that the jump is instantaneous):

$$\psi(t) = (v(t) - v_{\infty 1})/[T_2 - T_1]; \quad \text{ideal infinitesimal jump} \tag{1}$$

where $v_{\infty 1}$ is the equilibrium volume at T_1.

* As usual, the terms volume recovery and volume relaxation are used interchangeably

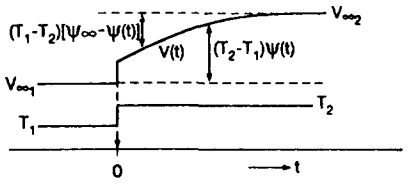

Figure 1 Definition of volume response function ψ

For an arbitrary temperature programme $T(t)$ starting at $t = 0$ from an equilibrium state at T_1, the Boltzmann integral (linearity principle) yields:

$$v(t) - v_{\infty 1} = \int_0^t \mathrm{d}T/\mathrm{d}\xi \psi(t-\xi)\mathrm{d}\xi \tag{2}$$

where ξ is an integration variable on the t-time scale.

Often[2], volume relaxation is characterized by the deviation from the equilibrium volume $v_{\infty 2}$ at final temperature T_2. According to equation (1) and *Figure 1*, this is given by:

$$v - v_{\infty 2} = [\psi_\infty - \psi(t)](T_1 - T_2) \tag{3}$$

(b) The linearity range for volume relaxation is limited to temperature jumps much smaller than 1°C[9]; for larger jumps, the relaxation is highly non-linear. The theory assumes that the non-linearities are due to accelerations/decelerations of the relaxation by a factor a (acceleration function) which only depends on temperature and volume (generalization of the principle of *thermo-rheological simplicity*). This implies that we can define *reduced time* λ given by*:

$$\lambda = \int_0^t a(\xi)\mathrm{d}\xi \tag{4}$$

where a depends on time via the changes in temperature and volume. Note that a is defined as increasing when relaxation is speeded-up (higher temperature or volume).

The reduced-time concept removes the non-linearities. On the λ-time scale, we have (cf. equation (2)):

$$v(\lambda) - v_{\infty 1} = \int_0^\lambda \mathrm{d}T/\mathrm{d}\zeta \psi(\lambda-\zeta)\mathrm{d}\zeta \tag{5}$$

where ζ is an integration variable on the reduced λ-time scale and ψ the response function defined by equation (1).

In ref. 7 the volume response was defined in terms of the actual volume changes. Kovacs used a normalized parameter $\delta = (v - v_\infty)/v_\infty$, where the abbreviation v_∞ denotes the equilibrium volume $v_{\infty 2}$ at final temperature T_2 (this abbreviation will be used frequently in this paper). To harmonize our notation with that of Kovacs, we define the response function:

$$\phi(\lambda) = [\psi_\infty - \psi(\lambda)]/v_\infty \tag{6}$$

Equation (3) then gives:

$$\delta(\lambda) = [v(\lambda) - v_\infty]/v_\infty = \phi(\lambda)[T_1 - T_2]; \quad \text{ideal jump} \tag{7}$$

It should be realized that ϕ is defined as the *theoretical response function for an ideal temperature jump*. Real volume relaxation is measured with dilatometers having thermal inertia. Thus, the actual temperature jumps are not ideal and the response may deviate from ϕ. To distinguish actual from ideal response the experimental response is denoted by:

$$\Phi(t) = \delta(t)/[T_1 - T_2] \tag{8}$$

In the sequel, Φ is considered as a function of t or λ; ϕ only as a function of λ. Equations (7) and (8) yield:

$$\Phi(\lambda) = \phi(\lambda); \quad \text{for ideal jumps} \tag{8a}$$

*2.2. Non-ideal temperature jumps**

We consider a non-ideal jump to final temperature T, starting from thermodynamic equilibrium at initial temperature T_0 (in the sequel, we use this notation instead of T_1 and T_2 as in *Figure 1*). Equations (5) and (6) yield:

$$\delta(\lambda) = -\int_0^{\lambda_\mathrm{d}} \mathrm{d}T/\mathrm{d}\zeta \phi(\lambda-\zeta)\mathrm{d}\zeta; \quad \lambda > \lambda_\mathrm{d} \tag{9}$$

where ζ is an integration variable in the λ-scale and λ_d the thermal equilibration time on the λ-scale (t_d is the equilibration time on the real t-time scale; λ_d can be related to t_d by equation (4)). Combining equations (8) and (9), we find:

$$\Phi(\lambda) = \int_0^{\lambda_\mathrm{d}} h(\zeta)\phi(\lambda-\zeta)\mathrm{d}\zeta; \quad \lambda > \lambda_\mathrm{d} \tag{10}$$

where the thermal transient is given by:

$$h(\lambda) = [\mathrm{d}T/\mathrm{d}\lambda]/(T - T_0) \tag{11}$$

Obviously

$$\int_0^{\lambda_\mathrm{d}} h(\zeta)\mathrm{d}\zeta = 1 \tag{12}$$

As usual in relaxation theory[12], we assume that $\phi(\lambda)$ is a positive, total monotonic decreasing function of λ. This means: $\phi \geq 0$, $\mathrm{d}\phi/\mathrm{d}\lambda \leq 0$, $\mathrm{d}^2\phi/\mathrm{d}\lambda^2 \geq 0$, etc. Such functions can be written as a sum of decaying positive exponentials (see also pp. 119–122 of ref. 7). Furthermore, since the dilatometer is subjected to a jump in the outside temperature, function h in equation (11) will be positive. Altogether, this means:

$$\Phi(\lambda) = \int_0^{\lambda_\mathrm{d}} h(\zeta)\phi(\lambda-\zeta)\mathrm{d}\zeta \geq \phi(\lambda)\int_0^{\lambda_\mathrm{d}} h(\zeta)\mathrm{d}\zeta = \phi(\lambda) \tag{13}$$

In the same way, we find: $\Phi(\lambda) \leq \phi(\lambda - \lambda_\mathrm{d})$, thus:

$$\phi(\lambda) \leq \Phi(\lambda) \leq \phi(\lambda - \lambda_\mathrm{d}) \tag{14}$$

or

$$\Phi(\lambda) = \phi(\lambda - \lambda_i); \quad \text{with } 0 \leq \lambda_i \leq \lambda_\mathrm{d} \tag{15}$$

in which λ_i *may vary* with λ.

In the same way, we find from equation (10):

$$-\dot{\Phi}(\lambda) = \int_0^{\lambda_\mathrm{d}} h(\zeta)[-\dot{\phi}(\lambda-\zeta)]\mathrm{d}\zeta; \quad \lambda > \lambda_\mathrm{d} \tag{16}$$

in which the dot denotes differentiation with respect to the argument. Since $-\dot{\phi}$ is positive and decreasing and h positive, we obtain as before:

$$-\dot{\phi}(\lambda) \leq -\dot{\Phi}(\lambda) \leq -\dot{\phi}(\lambda - \lambda_\mathrm{d}) \tag{17}$$

* In ref. 7, λ was called the effective time; the present name is used to avoid confusion with Kovacs's effective relaxation time τ_eff

* The results of Sections 2.2 and 2.3 are based on refs 10 and 11

or

$$\dot{\Phi}(\lambda) = \dot{\phi}(\lambda - \lambda_j); \quad \text{with } 0 \leq \lambda_j \leq \lambda_d \qquad (18)$$

where λ_j may vary with λ and be different from λ_i. Because of the total monotony (see above), similar formulae hold for all higher derivatives of Φ. Moreover, since $h(\zeta) > 0$ for cooling as well as for heating, equations (15) and (18) hold in both cases.

The difference between Φ (non-ideal jump) and ϕ (ideal jump) can be written as:

$$\Delta = \Phi(\lambda) - \phi(\lambda) = \phi(\lambda - \lambda_i) - \phi(\lambda) \approx -[\lambda_i/\lambda]\mathrm{d}\phi\mathrm{d}\ln\lambda$$

With equation (15), we obtain:

$$0 \leq \Delta \leq [\lambda_d/\lambda][-\mathrm{d}\phi/\mathrm{d}\ln\lambda] \qquad (19)$$

The rate of ϕ can be connected to that of Φ. Equation (17) gives:

$$-\mathrm{d}\Phi/\mathrm{d}\ln\lambda = -\lambda\dot{\Phi}(\lambda) \geq -\lambda\dot{\phi}(\lambda) = -\mathrm{d}\phi/\mathrm{d}\ln\lambda \qquad (20)$$

So, equation (19) can be replaced by:

$$0 \leq \Delta \leq [\lambda_d/\lambda][-\mathrm{d}\Phi/\mathrm{d}\ln\lambda] \qquad (21)$$

Consequently, if shift function $a(\delta)$ is known, we can calculate λ from t and $\delta(t)$, determine $\Phi(\lambda)$ and $\mathrm{d}\Phi/\mathrm{d}\ln\lambda$ and find the maximum difference, Δ, between non-ideal and ideal heating jumps. A (generally too large) upper bound for Δ can be found without having any detailed knowledge about shift function $a(\delta)$. Since, upon heating, δ and $a(\delta)$ increase with time, we have:

$$\lambda = \int_0^t a(\xi)\mathrm{d}\xi = a(t)\int_0^t [a(\xi)/a(t)]\mathrm{d}\xi \leq ta(t); \quad \text{heating} \qquad (22)$$

So, λ/t will be smaller than $a(t)$. The increase of a with time also implies (see equation (16) of ref. 1):

$$\lambda_d/\lambda \leq t_d/t; \quad \text{heating jumps} \qquad (23)$$

Furthermore we have the identity (see equation (4)):

$$\mathrm{d}\Phi/\mathrm{d}\ln t = t\mathrm{d}\Phi/\mathrm{d}t = ta(t)\mathrm{d}\Phi/\mathrm{d}\lambda = a(t)[t/\lambda]\mathrm{d}\Phi/\mathrm{d}\ln\lambda \qquad (24)$$

Combining equations (20), (22) and (24), and remembering that the time derivatives of ϕ and Φ are negative, we find:

$$-\mathrm{d}\Phi/\mathrm{d}\ln t \geq -\mathrm{d}\Phi/\mathrm{d}\ln\lambda \geq -\mathrm{d}\phi/\mathrm{d}\ln\lambda; \quad \text{heating} \qquad (25)$$

The first part of this inequality is due to the non-linearity of the volume-recovery process ($a(\delta)$ increases with time) the second to the non-ideality of the temperature jump. Combining equations (21), (23) and (25), we finally obtain:

$$0 \leq \Delta \leq [t_d/t][-\mathrm{d}\Phi/\mathrm{d}\ln t]; \quad \text{heating} \qquad (26)$$

which gives a direct estimate of Δ from the data on the t-time scale. If $a(\delta)$ increases strongly, Δ is overestimated correspondingly.

2.3. Course of λ, Φ and ϕ during volume relaxation

In a heating experiment, $a(\delta)$ increases with time; after quenching it decreases. Since $a(t) = \mathrm{d}\lambda/\mathrm{d}t$ (equation (4)), this leads to the λ vs t behaviour shown in *Figure 2a*. For ideal jumps, this translates into the Φ vs t behaviour

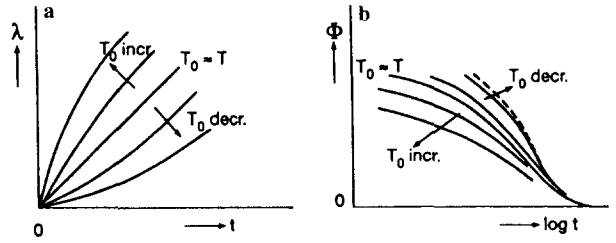

Figure 2 (a) Course of reduced time λ vs real time t after an ideal or non-ideal jump from thermodynamic equilibrium at T_0 to final temperature T. (b) Corresponding course of Φ vs $\log t$ for ideal jumps (—) and a non-ideal jump (- - -)

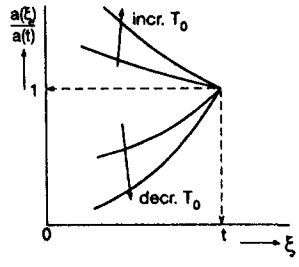

Figure 3 Course of $a(\xi)/a(t)$ vs ξ for ideal jumps from thermodynamic equilibrium at T_0 to final temperature T

shown in *Figure 2b*; equation (8) then yields:

$$\Phi(t) = \phi[\lambda(t)]; \quad \text{ideal jumps} \qquad (27)$$

For non-ideal jumps, Φ will be somewhat larger that ϕ, both for heating and cooling. In *Figure 2b*, the course for a non-ideal jump has been indicated by a dashed curve. *Figure 2b* shows that, for ideal jumps, the Φ vs $\ln t$ curves steepen with decreasing T_0 (heating) and flatten with increasing T_0 (cooling). This follows from equation (22), which yields:

$$\mathrm{d}\Phi/\mathrm{d}\ln\lambda/\mathrm{d}\Phi/\mathrm{d}\ln t = \lambda/[ta(t)] = [1/t]\int_0^t a(\xi)/a(t)\mathrm{d}\xi \qquad (28)$$

The course of $a(\xi)/a(t)$ is given schematically in *Figure 3*; the integral in equation (28) obviously increases with increasing T_0. Now consider jumps to the same final temperature T from different initial temperatures T_0. Since the jumps are ideal, a fixed (given) value of Φ implies a fixed value of ϕ (equation (27)) and thus fixed values of λ and $\mathrm{d}\Phi/\mathrm{d}\ln\lambda = \mathrm{d}\phi/\mathrm{d}\ln\lambda$. Consequently, the increase of the integral of equation (28) with increasing T_0 is accompanied by a decrease of $-\mathrm{d}\Phi/\mathrm{d}\ln t$.

3. TEST ON KOVACS'S δ VS t DATA

We will now test the theory on Kovacs's original volume-recovery curves for PVAc at 40°C (*Figure 4*). *Table 1* gives the δ-values read from a magnified version of *Figure 4*; the t-values are equidistant on a $\log t$ scale with a spacing of 0.1 decade. For reasons explained below, *Table 1* is restricted to the heating data and to times $t \geq 0.02$ h. *Figure 5* gives the Φ vs $\log t$ curves calculated from *Table 1*; the steepening with decreasing T_0 (*Figure 2b*) is clearly visible.

Testing of the theory means: (i) finding the proper shift function $a(\delta)$; (ii) calculating reduced time $\lambda(t)$ (equation (4)) for each δ vs t curve and constructing the $\Phi(\lambda) = \delta(\lambda)/(T_0 - T)$ vs λ curves; (iii) verifying whether

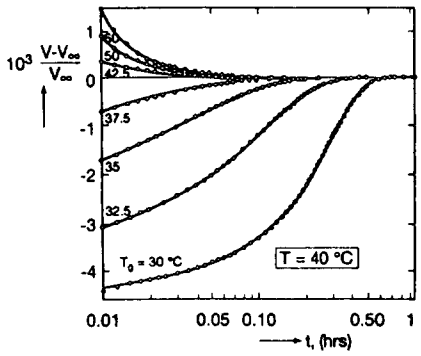

Figure 4 Volume recovery at $T = 40°C$ for PVAc after up- and down-quenches from various initial temperatures T_0; reproduced with permission from Figure 17 of ref. 2

Table 1 $10^3\,\delta$ vs t as read from *Figure 4*

		T_0 (°C)			
t (h)	$10 \log t$	37.5	35.0	32.5	30.0
0.0200	−1.70	−0.395	−1.269	−2.704	−4.174
0.0251	−1.60	−0.329	−1.132	−2.576	−4.122
0.0316	−1.50	−0.253	−0.977	−2.418	−4.033
0.0398	−1.40	−0.178	−0.799	−2.236	−3.944
0.0501	−1.30	−0.141	−0.645	−2.046	−3.838
0.0631	−1.20	−0.086	−0.487	−1.793	−3.704
0.0794	−1.10	−0.046	−0.349	−1.530	−3.546
0.1000	−1.00	−0.023	−0.227	−1.214	−3.342
0.1259	−0.90	−0.016	−0.135	−0.914	−3.082
0.1585	−0.80	−0.000	−0.053	−0.614	−2.697
0.1995	−0.70		−0.016	−0.340	−2.293
0.2512	−0.60		−0.000	−0.176	−1.756
0.3162	−0.50			−0.069	−1.144
0.3981	−0.40			−0.015	−0.565
0.5012	−0.30			−0.000	−0.174
0.6310	−0.20				−0.020
0.7943	−0.10				−0.000

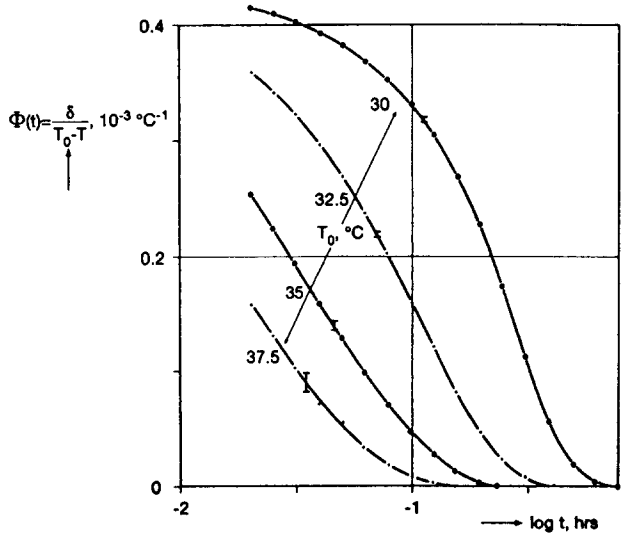

Figure 5 Φ vs $\log t$ for the heating data of *Figure 4*. Error bars denote the experimental accuracy in Φ of $\pm\epsilon/(T - T_0)$ with $\epsilon = 2 \times 10^{-5}$

the Φ vs λ curves obtained for different T_0's superimpose for λ-values much larger than λ_d. If superposition succeeds *within experimental error* $(\pm\epsilon = \pm 2 \times 10^{-5})$[1], the theory may be said to work.

As explained in ref. 1, the curves after cooling strongly depend on the non-ideal aspects of the quenching process. We *therefore restrict ourselves to the heating data, but even these are affected considerably by the non-ideality of the temperature jumps.*

3.1. The shortest reliable measuring time

According to Kovacs[13], thermal equilibration time t_d was about 0.02 h for Bekkedahl dilatomers in thermostats filled with water; for his other dilatometers and for oil baths, t_d was a factor of 1.5–3 larger. Kovacs's data indeed show deviations at short times, e.g. in *Figure 4*, the lowest curve (drawn by Kovacs) deviates by 6.5×10^{-5} from the experimental point at $t = 0.01$ h. Similar deviations are seen at other places[2,13,14]; these clearly reflect the non-isothermal conditions at short times.

In the above example, the volume deviation of 6.5×10^{-5} at 0.01 h corresponds to a temperature deviation of 0.3°C [in view of the short times, we use the short-time (glassy) expansivity $\alpha_g = 2.4 \times 10^{-4}$/°C from Table 1 of ref. 2]. The temperature jump being 10°C, we see that, after 0.01 h, the jump is completed for 97%.

The height of the mercury column (dilatometer reading) is determined by the average temperature in the dilatometer. For such cylindrical tubes, the average temperature varies with t according to a single exponential:

$$R = [T(t) - T]/[T_0 - T] \approx \exp(-t/\tau) \qquad (29)$$

for the last phase (last 30%) of the transient[15]; during the earlier phases, we need more terms of the series. With $R = 0.03$ and $t = 0.01$ h, we find $\tau = -0.01/\ln(0.03) = 0.01/3.5 = 2.9 \times 10^{-3}$ h = 10.2 s. This compares reasonably with the estimates made in ref. 16; for a cylindrical dilatometer (mercury–glass–polymer) with polymer filling of 50% and outer diameter of 1 cm, we calculated a τ of 13 s.

To get the volume within experimental error $(\pm\epsilon = \pm 2 \times 10^{-5})$, the deviation in temperature should be less than 0.083°C $(= \epsilon/\alpha_g = 2 \times 10^{-5}/2.4 \times 10^{-4})$. For a jump of 10°C, this requires that $t > 4.8\tau$; for smaller jumps the times required are slightly smaller. Between 0.01 and 0.02 h, t/τ increases from 3.5 to 7 and the temperature deviation reduces by a factor of $e^{3.5} = 33$. At 0.02 h, it will be much smaller than the required value of 0.083°C. So, Kovacs's claim of thermal equilibrium after 0.02 h looks quite reasonable. We therefore consider the points for $t \geq 0.02$ h as reliable and disregard those at shorter times.

3.2. Superposition of the Φ vs λ curves for data points which are hardly affected by the non-ideality of the temperature jump

The superposability is now tested as follows: we start with some reasonable function $\log a(\delta)$ and calculate λ vs t with equation (4) and the δ vs t data of *Table 1*. Next we plot Φ vs λ and check whether the curves for different T_0's superimpose. We take the following precautions:

- the deviation, Δ, due to non-ideal heating is estimated with equation (21). For λ_d we substitute the smallest λ value, viz. initial value $\lambda_1 = a(0.02\,\text{h}) \times 0.02$ h. This λ_1 is certainly greater than λ_d since t_d is less than 0.02 h and $a(0.02\,\text{h})$ exceeds the $a(t)$ values for $t < 0.02$ h. Since $\lambda_1 > \lambda_d$, the estimated Δ's are too large; so, we remain at the safe side.

- we only consider points for which the volume error $[\Phi - \phi](T - T_0) = \Delta(T - T_0)$, due to non-ideal heating, is less than $\epsilon = 2 \times 10^{-5}$; all other points are rejected.

For the shift function we use Kovacs's equation[1]:

$$\log a(\delta) = c\delta/[1 + d\delta] \quad (30)$$

and we optimize c and d. According to the free-volume model, d should be positive (if Doolittle's b-factor is taken as unity, we have $d = 1/f_T$, where f_T is the equilibrium free-volume fraction at T). For reasons which become clear later, we also consider negative d-values.

A simple PC-programme was written that uses the data of *Table 1* as input; for given c and d, the Φ vs λ curves then follow straightforwardly. Integration of equation (4) was done numerically in steps of 0.01 decade. Over each interval (0.01 decade), $a(t)$ was approximated by a power law, the power being found from c, d and the experimental δ-values. To get the δ-values for this narrow spacing (0.01 decade), the data of *Table 1* (spacing of 0.1 decade) were interpolated by 3-point forward differences on the $\log t$ scale (second degree polynomial).

The scatter around the mastercurve was calculated by the computer programme. The $\Phi(\lambda)$ curve obtained for $T_0 = 30°C$ was taken as reference; compared to the curves for other T_0's, it extends over the largest λ-interval and is the most accurate (note that errors in Φ decrease with increasing difference $T - T_0$). Next, the programme compares the $\Phi(\lambda)$ curves for other T_0's with the reference curve for $T_0 = 30°C$ and determines the differences. The error $\pm\epsilon$ in the δ-values leads to an error $\pm\epsilon/10$ in the Φ-values for the reference curve ($T_0 = 30°C$); for other T_0's, the errors in Φ are $\pm\epsilon/(T - T_0)$. To remain within experimental error, the difference between the $\Phi(\lambda)$ curve for T_0 and the reference curve must be less than $\pm\epsilon[1/10 + 1/(T - T_0)]$. In the computer programme, we multiplied each Φ-difference by $T - T_0$ in order to get the difference in terms of volume (Φ is volume/°C). To remain within experimental error, this difference should be less than $\pm\epsilon[1 + (T - T_0)/10] = \pm 1.25\epsilon$ for $T_0 = 37.5°C$ and $\pm 1.75\epsilon$ for $T_0 = 32.5°C$. In the computer programme we determined the maximum difference ($\Delta\Phi(T - T_0)$) for all T_0's simultaneously, so, we did not discriminate between points originating from different T_0's. As an average, *we therefore take* $+1.5\epsilon = +3 \times 10^{-5}$ *as the expected scatter in* Φ *due to the experimental errors in* δ.

The results are shown in *Figure 6*. The scatter is plotted vs d with c as a parameter. The horizontal dashed line at 3×10^{-5} is the experimental accuracy discussed above. We notice the following:

(1) For the *free-volume model*, d must be positive and the scatter remains above 5×10^{-5} (*Figure 6*). In this model, Doolittle's b-factor is often set equal to unity; this links d and c by[1]:

$$d = \sqrt{(2.303c)} \quad (31)$$

Using equation (31), we get the scatter curve of *Figure 7*. Obviously, the scatter is minimum for $c = 640$, which corresponds to $f_T = 1/d = 0.026$. These are quite usual values, close to those used to construct the mastercurve of Figure 9 of ref. 1 ($c = 600$; $f_T = 1/d = 0.027$) and also close to those used by Kovacs in drawing the dotted $\log a$ vs δ curve in Figure 6 of ref. 3 ($c = 670$ and $f_T = 1/d = 0.028$).

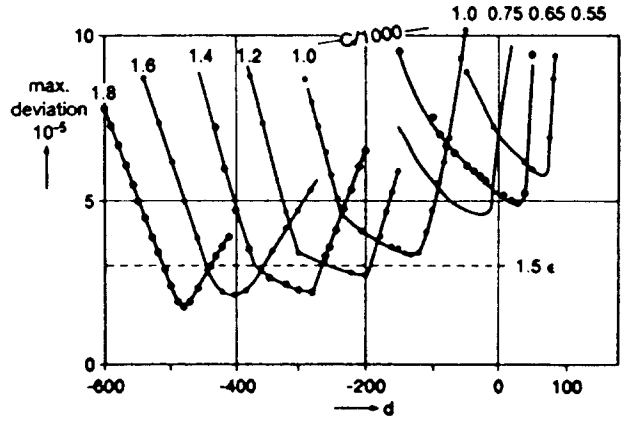

Figure 6 Maximum (absolute) deviation between the reference curve ($T_0 = 30°C$) and the $\Phi(\lambda)$ curves for $T_0 = 32.5$, 35 and 37.5°C; for explanation see text

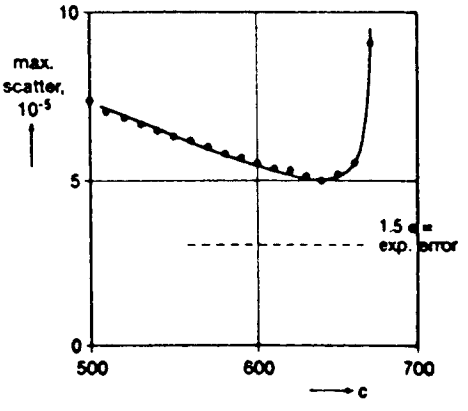

Figure 7 Maximum scatter in the mastercurves for the free-volume model with Doolittle's b-factor equal to unity [$d = \sqrt{(2.303c)}$]

The resulting mastercurve is shown in *Figure 8* (curve A). *Figure 6* reveals that a substantial reduction of the scatter is only possible with negative d-values. So, with the free-volume model (positive d's) a scatter of $\pm 5 \times 10^{-5}$ (curve A) is the best we can achieve; the scatter remains about 60% larger than expected from experimental error.

(2) *Negative* d*-values. Figure 6* shows that the scatter can be reduced below experimental error by taking negative d-values. For $c = 1000$ and $d = -130$ ($k = 1/d = -0.077$), the scatter drops to 3.4×10^{-5}, for $c = 1800$ and $d = -480$ ($k = 1/d = -0.00208$) to 1.7×10^{-5}. The corresponding mastercurves are shown in *Figure 8*; the one for $c = 1800$ is almost perfect. Our theory[7] does not make assumptions about shift function $a(\delta)$; so, negative d-values are admissible. Such values, however, violate the free-volume model and lead to the unusual variation of $\log a$ with δ shown in *Figure 9*. For the free-volume model, $\log a$ vs δ shows a slope that (slowly) increases with decreasing δ; for negative d values, we have the reverse. It should not be excluded that this (unusual) effect is real and related to Angell's[17] finding that, for inorganic glasses, the free-volume model breaks down just above T_g: approaching T_g from above, the rapid changes of viscosity with temperature (free-volume effect) terminate and the behaviour changes to Arrhenius (see also ref. 18).

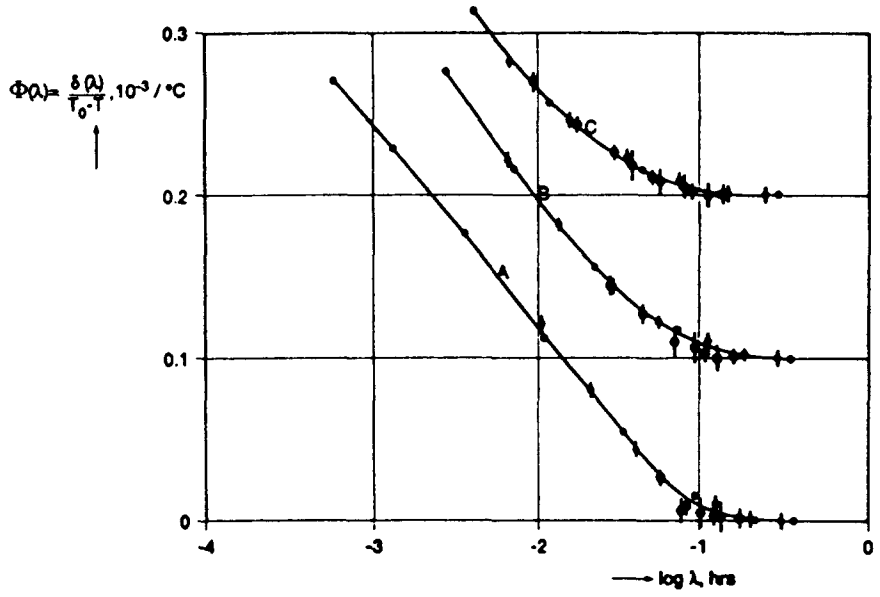

Figure 8 Mastercurves for $\Phi(\lambda)$, obtained as described in the text. Curve A: free-volume model with $b = 1$ ($d = \sqrt{(2.303c)}$), $c = 640$ and $1/d = 0.026$. Curve B: $c = 1000$ and $1/d = -0.077$; curve lifted by 0.1×10^{-3}. Curve C: $c = 1800$, $1/d = -0.00208$; curve lifted by 0.2×10^{-3}. The vertical bars give the errors $\pm\epsilon/(T - T_0)$ in Φ; the largest bars refer to $T_0 = 37.5°C$; the smallest to $T_0 = 32.5°C$ and the medium ones to $T_0 = 35°C$. The dots, without error bar refer to $T_0 = 30°C$; the size of the dots equals the error. The mastercurves B and C are within experimental error; for A the scatter exceeds experimental error by 60%

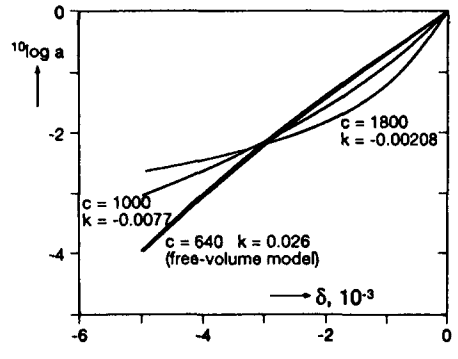

Figure 9 Log a vs δ relations as used in the construction of the mastercurves of *Figure 8*; the c and $k = 1/d$ parameters are indicated

Conclusion. The theory works; we can construct mastercurves for $\Phi(\lambda)$ within experimental error. However, the required $\log a$ vs δ relationships are not compatible with the free-volume model. With this model, the scatter remains 60% larger than as expected from experimental accuracy.

Remarks. (a) The negative d values should not be considered as some peculiar result of the superposition method. In fact, the unusual shifting behaviour directly follows from the experimental data. Let us assume for a moment that we have ideal temperature jumps. According to equations (4) and (8), the volume relaxation rate is then given by:

$$d\Phi/dt = a(\delta)d\Phi/d\lambda = a(\delta)d\Phi/d\lambda; \quad \text{ideal jumps} \quad (32)$$

Let us now compare points at equal $\Phi = \delta/(T_0 - T)$ originating from different T_0's. Let the rates, $d\Phi/dt$, be given by $r = r_1, r_2, ..$.etc. and the δ's by $\delta = \delta_1, \delta_2, \ldots$, etc. Equal Φ's imply equal ϕ's, λ's and thus equal rates $d\Phi/d\lambda$. So, at equal Φ, rate $d\Phi/dt$ varies in proportion to $a(\delta)$ (equation (32)). Therefore, by plotting $\log r$ vs the corresponding δ (r_1 vs δ_1, etc.) we directly obtain $\log a$, except for some constant that can be found from the condition that $\log a = 0$ for $\delta = 0$. So, *for ideal jumps, the shift function directly follows from the experimental data*[10,11]. Following this procedure and taking care of the non-ideal heating effects and the (large) errors in rate at $\delta \to 0$ (see ref. 1), we indeed found a $\log a$ vs δ curve with a slope increasing with δ (negative d-value). However, with Kovacs's data (*Figure 4*), the accuracy of this method is limited; for small t-values (large δ's), the rates are influenced by the non-ideal heating effects, for long times, the rates are unreliable because of the small δ's[1].

(b) Unfortunately, Kovacs's data were all in the non-linear range (considerable variation of shift factor $\log a$). Consequently, $\log a(\delta)$ and $\phi(\lambda)$ cannot be determined independently. The resulting $\phi(\lambda)$ depends on the $\log a(\delta)$ relationship chosen and we cannot decide which of the three $\log a(\delta)$ relations of *Figure 9* is the best, although negative d-values seem preferable. This ambiguity can be removed by additional volume-relaxation tests with very small temperature jumps ($\ll 1°C$) as described by Goldbach[9]. The non-linear effects then (almost) disappear; shift factor a remains about unity, λ becomes equal to t and the experimental $\Phi(t)$ equals the theoretical response function $\phi(\lambda)$. So, $\phi(\lambda)$ can be determined unambiguously; shift function $\log a$ then follows from the non-linear recovery at larger amplitudes.

3.3. The effect of non-ideal heating on the relaxation curves

As can easily be verified, *Figure 5* contains 2–3 times more data points than each of the mastercurves of *Figure 8*. The missing points ($\frac{1}{2} - \frac{2}{3}$ of the total) are those rejected because the effect of non-ideal heating, Δ, (see eqn 21) exceeds experimental error. The inevitable conclusion follows that *the original data (Figures 4 and 5) must have been affected considerably by these non-idealities*. An illustration is given in *Figure 10*. It refers to mastercurve A of *Figure 8* (free-volume model), but now,

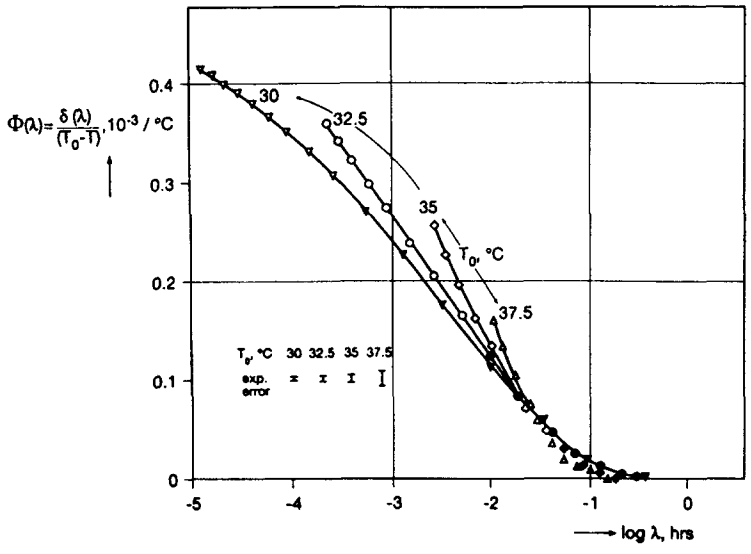

Figure 10 Mastercurves for $\Phi(\lambda)$ as obtained with the free-volume model (as curve A of *Figure 8*; $c = 640$ and $1/d = 0.026$). Now, all data points of *Figure 5* are given, including those (open symbols; rejected in *Figure 8*) affected by the non-ideality of the heating process by more than experimental error (equation (21)). The filled symbols are the points of *Figure 8*. Error bars ($\pm\epsilon/(T - T_0)$) with $\epsilon = 2 \times 10^{-5}$ are given for the different T_0's. For further explanation see text

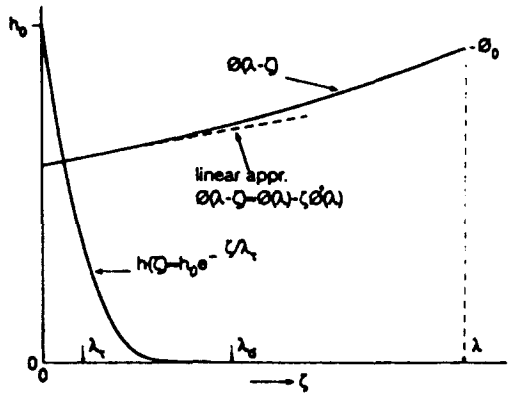

Figure 11 On the evaluation of the integral of equation (10); for explanation see text

all data points of *Figure 5* are included. Clearly, the $\Phi(\lambda)$ curve for T_0's of 32.5–37.5°C lags behind that for $T_0 = 30$°C. We return to these differences in the next section; here, it suffices to say that *the non-idealities in the heating process have a large effect on volume-recovery. If ignored*[4,19–30]*, the data are spoiled and little can be concluded about the applicability of the phenomenological volume-recovery theory.*

It should be realized that the distinction between open and closed symbols in *Figure 10* was made on the basis of equation (21), i.e. before the mastercurves of *Figure 8* were constructed. So, we did not reject points because of bad fitting; the choice was made independently and beforehand. In this respect, it is gratifying that the curves for 30° and 32.5°C roughly merge where the symbols change from open to closed (32.5°C curve). For $T_0 = 35°$ and 37.5°C, merging occurs earlier which reflects the fact that equation (21) overestimates the errors due to non-ideal heating, particularly for higher T_0's (next section).

3.4. Correction for the non-ideal heating effects

We start from equation (10) which shows that $\Phi(\lambda)$ is some average of ϕ over the interval between $\lambda - \lambda_d$ and λ, the weighing function being $h(\zeta)$. We further have:

$$t \geq t_d = 0.02\,\text{h} \approx 7\tau \tag{33}$$

where $\tau \approx 10$ s denotes the time constant of the thermal transient (see equation (29)). In a heating experiment, $a(\delta)$ increases with t, thus:

$$\lambda \geq \lambda_d \geq 7\lambda_\tau \tag{34}$$

where λ_τ is the λ-value corresponding with $t = \tau$.

As shown in *Figure 11*, $h(\zeta)$ decreases rapidly with ζ. On the t-time scale, $h(t)$ approximately obeys the exponential form of eqn (29). Since $a(\delta)$ increases with t, the λ vs t plot is upwardly curved (*Figure 2a*); so, the decrease in h is even sharper on the λ-time scale than on the t-time scale. As a rough estimate we write:

$$h(\zeta)/h_0 = \exp(-\zeta/\lambda_\tau) \tag{35}$$

where h_0 follows from equation (12):

$$h_0 = 1/\{\lambda_\tau[1 - \exp(-\lambda_d/\lambda_\tau)]\} \approx 1/\lambda_\tau \tag{36}$$

in which the exponential is about zero because of equation (34).

For $\zeta = \lambda_d$, h/h_0 is less than $e^{-7} = 0.0009$; for $\zeta = \frac{1}{2}\lambda_d$, h/h_0 is less than $e^{-3.5} = 0.03$. So, in equation (10), most of the contribution to $\Phi(\lambda)$ originates from ζ-values smaller than $\frac{1}{2}\lambda_d$. For such small ζ-values we may use the approximation shown in *Figure 11*:

$$\phi(\lambda - \zeta) \approx \phi(\lambda) - \zeta\dot{\phi}(\lambda) \tag{37}$$

Substitution into equation (10) yields:

$$\Phi(\lambda) \approx \phi(\lambda) - e_1\dot{\phi}(\lambda) \approx \phi(\lambda - e_1) \tag{38}$$

where e_1 is a constant given by:

$$e_1 = \int_0^{\lambda_d} \zeta h(\zeta)\,\mathrm{d}\zeta \tag{39}$$

Equation (38) resembles equation (15), however e_1 is a constant whilst λ_i may vary with λ. Equation (38) shows that *non-ideal heating causes a constant shift* e_1 *on the linear λ-time scale*; on the log time scale, the displacement decreases with increasing λ.

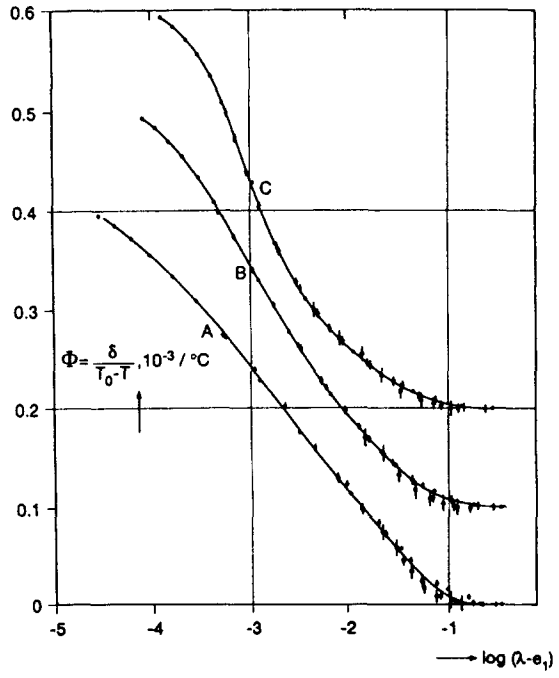

Figure 12 As *Figure 8*, but now corrected for the non-ideal heating effects (equation (38)) and all points with $\lambda \geq 2.5\lambda_1$ included (remember that $\lambda_1 \geq \lambda_d$; note that we took the slightly larger parameter of 2.5 instead of the value of 2 discussed below). The points for $T_0 = 30°C$ were not corrected; for the other T_0's, the correction e_1 was determined by shifting the data to optimum fit. A, B and C have the same meaning as in *Figure 8*; as before curves B and C were lifted by 0.1 and 0.2×10^{-3}, respectively. For $T_0 = 32.5$, 35 and 37.5°C, the e_1 values (in h) were, respectively, 0.002, 0.0023, 0.00043 for A; 0.004, 0.0009 and 0 for B; and 0.004, 0, and −0.00024 for C

The accuracy of equation (38) was investigated by considering model functions for $\phi(\lambda)$, i.e. the KWW function $\phi(\lambda) = \phi_0 \exp(-(\lambda/\tau_0)^{\beta})$. We varied β between 0.2 and 1 and λ_τ/τ_0 between 0.01 and 100. We further used equation (35) to describe the heating process. The errors in equation (38) turned out to be less than $0.002\phi_0$ for $\lambda \geq 2\lambda_d$. Since $\phi_0 \approx 4.5 \times 10^{-4}/°C$ (cf. *Figure 10* and remember that ϕ_0 equals $\Delta\alpha = 4.5 \times 10^{-4}/°C$ [2]) the errors in ϕ will be less than $10^{-6}/°C$. In the experiments of *Figure 10* the maximum value of $T - T_0$ was 10°C, so the experimental error in Φ was $\pm\epsilon/10 = \pm 2 \times 10^{-6}$ which is larger than the approximation error. Consequently, *the first-order approximation (equation (38)) will be within experimental error for* $\lambda \geq 2\lambda_d$.

The experimental results are shown in *Figure 12*; the *c*- and *d*-values were the same as *Figure 8* and the correction factors e_1 are given in the figure caption. The fit is quite good, which means that *the (rather large) effects of non-ideal heating can be described satisfactorily by the theory.*

Corollary. Equation (38) also explains why the effects of non-ideal heating could be neglected in constructing the mastercurve of Figure 9 of ref. 1. The quantities plotted against each other were $y = \tau'_{\text{eff}} = a(\delta)\tau_{\text{eff}}$ (vertical axis) and $x = \delta/[T_0 - T]$ (horizontal axis) where τ_{eff} is defined[1] as $-\delta/[d\delta/dt]$. For the heating experiments, equations (8) and (38) give:

$$x = \Phi(\lambda) = \phi(\lambda - e_1) \tag{40}$$

$$\begin{aligned} 1/y &= -[d\ln(-\delta)/dt]/a(\delta) = -d\ln\Phi/d\lambda \\ &= -d\ln\phi(\lambda - e_1)/d\lambda \\ &= -d\ln\phi(\lambda - e_1)/d(\lambda - e_1) \end{aligned} \tag{41}$$

where the change from $d../d\lambda$ to $d../d(\lambda - e_1)$ is allowed because e_1 is constant during volume relaxation (at least for $\lambda > 2\lambda_d$). With:

$$\lambda' = \lambda - e_1 \tag{42}$$

Equations (40) and (41) change into:

$$x = \phi(\lambda') \tag{43}$$

$$1/y = -d\ln\phi(\lambda')/d\lambda' \tag{44}$$

In the Appendix of ref. 1 we showed that there is a unique relationship between $-d\ln\phi/d\lambda$ and ϕ:

$$-d\ln\phi(\lambda)/d\lambda = F\{\phi(\lambda)\} \tag{45}$$

in which F is some function. The same relationship of course holds for $\phi(\lambda')$ and $d\ln\phi(\lambda')/d\lambda'$, i.e. for the experimental quantities x and $1/y$ (see equations (43) and (44)). So, the effect of non-ideal heating on the y vs x plot (Figure 9 of ref. 1) disappears by virtue of the constancy of e_1.

4. DISCUSSION AND CONCLUSIONS

The following conclusions can be drawn: (1) The volume-recovery curves (δ vs t; PVAc, 40°C; heating) from which Kovacs calculated the effective relaxation time τ_{eff} can be described by the phenomenological volume-recovery theory within experimental error ($\pm 2 \times 10^{-5}$). (2) The volume-recovery curves are strongly influenced by the non-ideality of practical temperature jumps (thermal transients lasting 50–70 s), even for heating. (3) The deviations due to non-ideal heating can be described by the theory.

So, the present results support the conclusion of ref. 1 that there is nothing paradoxical in Kovacs's volume-recovery data. It is also clear now why the many attempts[4,19–30] to describe Kovacs' data quantitatively had limited success. In all cases the long-time errors in τ_{eff}[1] as well as the short-time deviations due to non-ideal heating were neglected. This spoils the data and no definitive conclusions could be drawn about the applicability of the phenomenological theory.

A final remark concerns the question whether the original δ vs t (*Figure 4*) data can be reproduced from shift function $\log a(\delta)$ and response function $\phi(\lambda)$ of *Figures 8* and *9*. In view of the strong non-linear effects this is not self-evident; for a non-linear process, success in one direction does not automatically guarantee success in the reverse direction. With own data on polystyrene, this two-way analysis has been made long ago[11]. Functions $\log a(\delta)$ and $\phi(\lambda)$ were determined as described in the present paper; from this, we could successfully describe the volume recovery on real t-time scale. However, the non-idealities in the temperature jumps were not corrected for, so the check was limited to $t \gg t_d$. We wish to perform this two-way comparison with Kovacs's accurate data and take the real thermal transients into account, also for cooling. This work is reserved for a future paper.

REFERENCES

1. Struik, L. C. E., *Polymer*, 1997, **18**, 4677.
2. Kovacs, A. J., *Fortschr. Hochpolym. Forsch.*, 1964, **3**, 394.
3. Kovacs, A. J., Hutchinson, J. M. and Aklonis, J. J., in *Structure*

of Non-Crystalline Solids, ed. P. H. Gaskell. Taylor & Francis, London, 1977, p. 153.
4. Kovacs, A. J., Aklonis, J. J., Hutchinson, J. M. and Ramos, A. R., *J. Polym. Sci. (Phys.)*, 1979, **17**, 1097.
5. Gardon, R. and Narayanaswamy, O. S., *J. Am. Ceram. Soc.*, 1970, **53**, 380.
6. Narayanaswamy, O. S., *J. Am. Ceram. Soc.*, 1971, **54**, 491.
7. Struik, L. C. E., *Physical Aging of Amorphous Polymers and Other Materials*. Elsevier, Amsterdam, 1977, pp. 117–122.
8. Struik, L. C. E., *Internal Stresses, Dimensional Instabilities and Orientation Effects in Plastics*. Wiley, Chichester, 1990, p. 26.
9. Goldbach, G. and Rehage, G., *Rheol. Acta*, 1967, **6**, 30.
10. Struik, L. C. E., Intern. Rep., Central Laboratory TNO, M70/132, M70/141, M70/142 and M70/162 (June–Aug 1970; in Dutch).
11. Struik, L. C. E., 'Volume Relaxation and Related Phenomena in Amorphous Polymers', Internal Stress Project, Technical Report No. 20, MRPI-74/56, Central Laboratory TNO, 17 July 1974.
12. Schwarzl, F. R. and Struik, L. C. E., *Adv. Mol. Relaxation Proc.*, 1967/68, **1**, 201.
13. Kovacs, A. J., Thesis Fac. Sci., Paris, 1954.
14. Kovacs, A. J., *J. Polym. Sci.*, 1958, **30**, 131.
15. Carlslaw, H. S. and Jaeger, J. C., *Conduction of Heat in Solids*. Oxford University Press, Oxford, 1947.
16. Struik, L. C. E., 'Het Dynamisch gedrag van dilatometers', Internal Report Central Laboratory TNO, D 62/60, 29-10-1962 (in Dutch).
17. Angell, C. A., in *Relaxation of Complex Systems*, ed. K. L. Ngai and G. B. Wright. Office of Naval Research, Arlington, USA, 1984, p. 3.
18. Crest, G. S., and Cohen, M. H., in *Adv. Chemical Physics*, Vol. 48, ed. I. Prigogine and S. A. Rice. Wiley, New York, 1981, p. 455.
19. McKenna, G. B., in *Comprehensive Polymer Science*, Vol. 2, Polymer Properties, ed. C. Booth and C. Price. Pergamon, Oxford, 1989, Chap. 10, p. 311.
20. Hutchinson, J. M., *Plastics, Rubber Compos. Proc. Appl.*, 1993, **20**, 187.
21. Hutchinson, J. M., *Prog. Polym. Sci.*, 1995, **20**, 703.
22. Chow, T. S., *J. Polymer Sci. (Phys)*, 1984, **22**, 699.
23. Chow, T. S., *Macromolecules*, 1984, **17**, 911.
24. Bendler, J. and Ngai, K. L., *Macromolecules*, 1984, **17**, 1174.
25. Rendell, R. W., Ngai, K. L., Fong, G. R. and Aklonis, J. J., *Macromolecules*, 1987, **20**, 1070.
26. Robertson, R. E., Simha, R. and Curro, J. G., *Macromolecules*, 1984, **17**, 911; 1985, **18**, 2239.
27. Matsuoka, S., Williams, G., Johnson, G. E., Anderson, E. W. and Furukawai, T., *Macromolecules*, 1985, **18**, 2652.
28. Robertson, R. E., *J. Polym. Sci. (Symposia)*, 1978, **63**, 173.
29. Robertson, R. E., *J. Polym. Sci (Phys.)*, 1979, **17**, 579.
30. Robertson, R. E., *Macromolecules*, 1985, **18**, 953.